



## Nonlinear Phenomena of Graphene Surface Waves due to Carrier Density Fluctuations

**Stamatios Amanatiadis<sup>1</sup> and Nikolaos Kantartzis<sup>1</sup>**

<sup>1</sup>Aristotle University of Thessaloniki, Dept. of Electrical & Comp. Eng., GR-54124, Thessaloniki, Greece  
samanati@auth.gr

**Abstract** – Rapid fluctuations of graphene carrier density due to strongly confined surface waves and the subsequent nonlinear response are studied in this work. Initially, the influence of the carrier density on graphene chemical potential is investigated thoroughly and a properly modified FDTD algorithm is introduced to evaluate the dynamically varied graphene surface conductivity. Numerical results highlight a considerable second-order nonlinearity besides the standard third-order one.

### I. INTRODUCTION

Various researchers have been attracted by graphene, the truly two-dimensional (2D) carbon allotrope, because of its exotic properties and universal applicability. Specifically, its finite conductivity, despite the negligible thickness, generates interesting phenomena, such as the ability to support strongly confined surface plasmon polariton (SPP) waves at the far-infrared regime [1]. Moreover, a significant third-order nonlinear electromagnetic response is observed at this spectrum, leading to frequency up-conversion and absorption saturation features [2, 3]. As anticipated, the nonlinear phenomena augment as the electromagnetic wave intensity is drastically increased, while graphene fundamental parameters, like the chemical potential and scattering rate, have, also, a noteworthy influence on this behavior.

Generally, graphene attributes are considered constant; an accurate fact for the majority of the analyses. However, the combination of the strong confinement of surface waves with the required intensity for nonlinear response is able to slightly alter the carrier density on graphene. As an immediate consequence, fluctuations of the chemical potential are observed, hence yielding a dynamic response of additional nonlinear features. To this end, it is the purpose of this paper to systematically investigate this complex phenomenon by means of a flexible finite-difference time-domain (FDTD) scheme in order to highlight its significance in the design of graphene plasmonic apparatuses. Initially, the 2D conductivity of the medium is described along with the connection of the chemical potential to carrier density. Then, a dynamic update model for the FDTD algorithm is proposed, where at each time-step the surface charge owing to electric displacement boundary conditions is incorporated into the graphene carrier density. Numerical results indicate a noticeable second-order nonlinearity of the SPP wave propagation, supplementary to the fundamental third-order one, due to the carrier density rapid fluctuations.

### II. THEORETICAL ASPECTS

Throughout our analysis, graphene is deemed an infinitesimally thin material characterized in terms of its surface conductivity. The latter is influenced by the fundamental graphene attributes, namely the chemical potential  $\mu_c$  and the scattering rate  $\Gamma$ . Furthermore, a low temperature is assumed, namely  $k_B T \ll |\mu_c|$  with  $k_B$  the Boltzmann constant, while the frequency range is up to the far-infrared regime, where the intraband transitions dominate. Finally, graphene's conductivity is split into a linear,  $\sigma^{(1)}$ , and a nonlinear term,  $\sigma^{(3)}$ , accurately evaluated, assuming monochromatic radiation, by the compact expression of [3]

$$\sigma_{\text{intra}}^{(1)}(\omega) = \frac{\sigma_0^{(1)}}{j\omega + 2\Gamma}, \quad \sigma_0^{(1)} = \frac{e^2 |\mu_c|}{\pi \hbar^2}, \quad (1)$$

$$\sigma_{\text{intra}}^{(3)}(\omega) = \frac{\sigma_0^{(3)}}{(j\omega + \Gamma)(j\omega + \frac{\Gamma}{2})(j\omega + \frac{\Gamma}{3})}, \quad \sigma_0^{(3)} = -\frac{e^4 u_F^2}{8\pi |\mu_c| \hbar^2}, \quad (2)$$

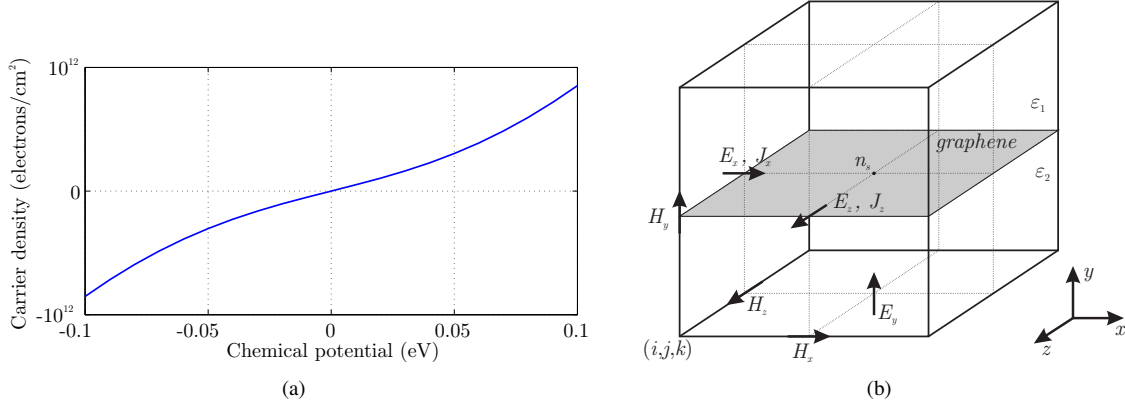


Fig. 1: (a) Carrier density on graphene versus chemical potential and (b) modified Yee cell including graphene's contribution as a surface current.

where  $e$  is the electron charge,  $\hbar$  the reduced Planck constant and  $u_F = 9.5 \times 10^6$  m/s the graphene Fermi velocity. It is evident, now, that the surface conductivity is significantly influenced by the chemical potential through the frequency-independent terms  $\sigma_0^{(1)}$  and  $\sigma_0^{(3)}$ . Additionally, it should be stressed that the chemical potential is efficiently adjusted via a constant electrostatic bias field that alters the carrier density  $n_s$  on graphene. The latter is computed through the boundary conditions on the 2D medium and particularly in terms of the discontinuity of electric displacement  $D_n^+ - D_n^- = en_s$ , whereas it is connected to the chemical potential by means of [1]

$$n_s = \frac{2}{\pi(\hbar u_F)^2} \int_0^\infty E [f_d(E) - f_d(E + 2\mu_c)] dE, \quad (3)$$

with  $f_d(E)$  the Fermi-Dirac distribution. Conventionally, the constant electrostatic bias field is several orders of magnitude larger than the propagating wave's one, thus, the carrier density can be safely considered as steady. Nevertheless, the emergence of standard third-order nonlinear characteristics requires stronger induced harmonic fields and local carrier density fluctuations are likely to arise. As a result, the chemical potential and graphene's surface conductivity are, also, influenced dynamically, especially at lower bias field values as illustrated in Fig. 1a.

The abovementioned case is considered in this paper and a properly modified FDTD algorithm is employed [4]. Particularly, both first and third-order responses of graphene are plugged into the FDTD algorithm as the sum of a linear,  $\vec{J}_{gr}^l$ , and a non-linear,  $\vec{J}_{gr}^{nl}$ , equivalent surface current, i.e.

$$\vec{J}_{gr} = \vec{J}_{gr}^l + \vec{J}_{gr}^{nl} = \frac{\sigma_0^{(1)}}{j\omega + 2\Gamma} \vec{E} + \frac{\sigma_0^{(3)}}{(j\omega + \Gamma)(j\omega + \frac{\Gamma}{2})(j\omega + \frac{\Gamma}{3})} |\vec{E}|^2 \vec{E}, \quad (4)$$

However, an additional modification is introduced to locally vary the chemical potential and the frequency-independent terms  $\sigma_0^{(1)}$ ,  $\sigma_0^{(3)}$  at each time-step via the updated local carrier density, namely

$$n_s|_{i+\frac{1}{2},j,k-\frac{1}{2}}^n = \frac{\varepsilon_1 E_y|_{i+\frac{1}{2},j+1,k-\frac{1}{2}}^n - \varepsilon_2 E_y|_{i+\frac{1}{2},j,k-\frac{1}{2}}^n}{e}, \quad (5)$$

where  $\varepsilon_1$  and  $\varepsilon_2$  are the superstrate and substrate dielectric permittivity, respectively. Note that the location of the surface current components are identical to the electric field ones, as depicted in Fig. 1b, while the local carrier density is calculated at the cell's center, thus a straightforward averaging between adjacent cells is required.

### III. NUMERICAL RESULTS AND CONCLUSION

In our simulations, graphene is located at the  $xz$ -plane with a chemical potential  $\mu_c = 0.1$  eV and a scattering rate  $\Gamma = 0.33$  meV, while the excitation, having an amplitude of  $2.5$  V/ $\mu$ m, is perpendicular to the material's surface

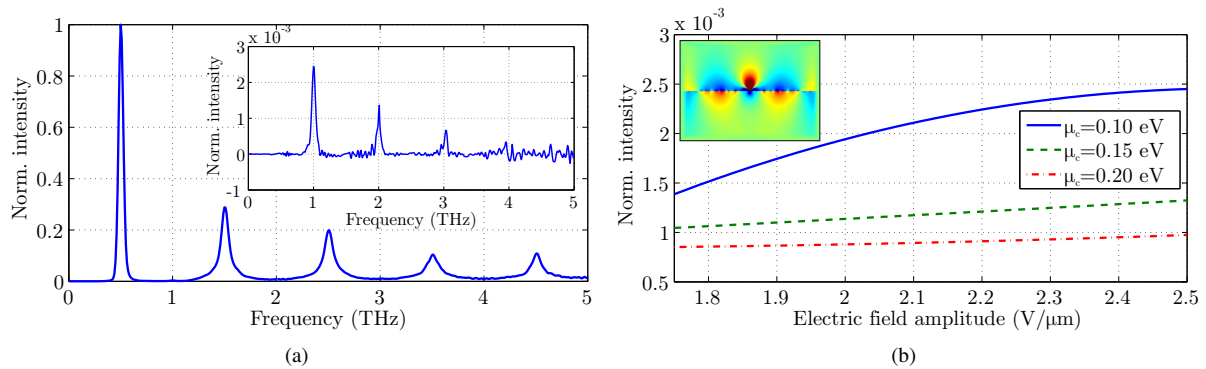


Fig. 2: (a) Surface wave intensity, normalized to the fundamental frequency. Inlet graph: Surface wave intensity due to carrier density nonlinearity. (b) Second-harmonic surface wave intensity versus electric field amplitude. Inlet graph: time-domain electric field distribution.

and it is nearly monochromatic with a central frequency at 0.5 THz. Note that the cell size is selected significantly lower than the wavelength, specifically  $\lambda/160$ , in order to guarantee the propagation of higher harmonics.

One preliminary observation of the results in Fig. 2a indicates the standard third-order response. Nonetheless, a second-order nonlinearity, also, appears; being more evident when subtracting the intensity due to the conventional algorithm, i.e. the one without a dynamic variation of the carrier density in (5). Although the strength of even harmonics is almost 1% that of the odd ones, it should be taken into consideration in the case of plasmonic device design. It is worth to mention that the intrinsic SPP propagation losses are counteracted via an appropriate time gain compensation procedure. Moreover, Fig. 2b unveils that the second-harmonic augments for larger excitation amplitudes and lower chemical potential values. The latter is to be expected, since the carrier density, attributed to the electrostatic bias, reduces as well, and the fluctuation is more likely to appear.

#### ACKNOWLEDGEMENT

This research is co-financed by Greece and the European Union (European Social Fund – ESF) through the Operational Programme “Human Resources Development, Education and Lifelong Learning»” in the context of the project “Reinforcement of Postdoctoral Researchers – 2nd Cycle” (MIS-5033021), implemented by the State Scholarships Foundation (IKY).



Operational Programme  
Human Resources Development,  
Education and Lifelong Learning  
Co-financed by Greece and the European Union



#### REFERENCES

- [1] G. W. Hanson, “Dyadic Green’s functions for an anisotropic, non-local model of biased graphene,” *IEEE Transactions on antennas and propagation*, vol. 26, no. 3, p. 747-757, 2008.
- [2] G. Xing, H. Guo, X. Zhang, T. C. Sum, and C. H. A. Huan, “The physics of ultrafast saturable absorption in graphene,” *Optics express*, vol. 18, no. 5, p. 4564-4573, 2010.
- [3] S. A. Mikhailov, “Quantum theory of the third-order nonlinear electrodynamic effects of graphene,” *Physical Review B*, vol. 93, no. 8, p. 085403, 2016.
- [4] S. A. Amanatiadis, T. Ohtani, T. T. Zygidis, Y. Kanai, and N. V. Kantartzis, “Modeling the third-order electrodynamic response of graphene via an efficient finite-difference time-domain scheme,” *IEEE Transactions on Magnetics*, vol. 26, no. 1, p. 1-4, 2019.